ACS APPLIED MATERIALS & INTERFACES

Research Article

www.acsami.org

# Preparation and Characterization of Aloe Vera Blended Collagen-Chitosan Composite Scaffold for Tissue Engineering Applications

Panneerselvam Jithendra,[†] Abraham Merlin Rajam,[†] Thambiran Kalaivani,[†] Asit Baran Mandal,[‡] and Chellan Rose*[,†]

[†]Department of Biotechnology and [‡]Chemical Sciences Division, CSIR-Central Leather Research Institute, Chennai 600020, India

Supporting Information

**ABSTRACT:** Collagen−Chitosan (COL-CS) scaffolds supplemented with different concentrations (0.1−0.5%) of aloe vera (AV) were prepared and tested in vitro for their possible application in tissue engineering. After studying the microstructure and mechanical properties of all the composite preparations, a 0.2% AV blended COL-CS scaffold was chosen for further studies. Scaffolds were examined by Fourier transform infrared spectroscopy (FT-IR), differential scanning calorimetry (DSC), and thermogravimetry analysis (TGA) to understand the intermolecular interactions and their influence on the thermal property of the complex composite. Swelling property in phosphate buffered saline (pH 7.4) and in vitro biodegradability by collagenase digestion method were monitored to assess the stability of the scaffold in a physiological medium in a hydrated condition, and to assay its resistance against enzymatic forces. The scanning electron microscope (SEM) image of the scaffold samples showed porous architecture with gradual change in their morphology and reduced tensile properties with increasing aloe vera concentration. The FTIR spectrum revealed the overlap of the AV absorption peak with the absorption peak of COL-CS. The inclusion of AV to COL-CS increased the thermal stability as well as hydrophilicity of the scaffolds. Cell culture studies on the scaffold showed enhanced growth and proliferation of fibroblasts (3T3L1) without exhibiting any toxicity. Also, normal cell morphology and proliferation were observed by fluorescence microscopy and SEM. The rate of cell growth in the presence/absence of aloe vera in the scaffolds was in the order: COL-CS-AV > COL-CS > TCP (tissue culture polystyrene plate). These results suggested that the aloe vera gel-blended COL-CS scaffolds could be a promising candidate for tissue engineering applications.

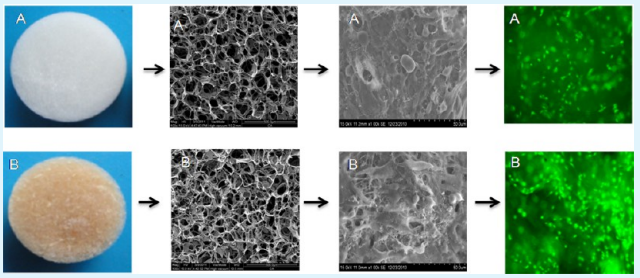


**KEYWORDS:** *collagen, chitosan, aloe vera, scaffold, tissue engineering*

## 1. INTRODUCTION

Tissue engineering is an emerging field offering new perspective in treatment by reconstructing the damaged or diseased organs. In this approach, a three-dimensional (3D) matrix generally serves as a template for host infiltration and physical support to guide the growth, differentiation, and proliferation of cells into the targeted functional tissue or organ.[1,2] This matrix, preferably a biomaterial, also called a scaffold, should be biocompatible with appropriate surface chemistry for cell attachment and proliferation, should have uniformly interconnected pores to facilitate infiltration and vascularization and controlled biodegradability with adequate mechanical properties to favor the tissue formation with structural integrity during remodeling of implants.[3,4] The scaffolds are commonly fabricated by synthetic and natural polymer such as collagen, chitosan, hyaluronic acid, etc. Among the synthetic polymers, aliphatic polyester like poly glycolic acid (PGA), poly lactic acid (PLA), poly lactic-co-glycolic acid (PLGA), polycaprolactone (PCL), etc., are widely used in tissue engineering because of their biodegradable nature.[5] However, the cell−material interactions are limited because of the poor cytocompatibility. In recent years, several surface modification techniques are focused to improve the biocompatibility without altering its bulk property.[6] The scaffolds are fabricated through various processing techniques such as conventional and novel method (Rapid prototype method). The conventional methods are solvent casting/particulate leaching, phase separation, gas foaming, and freeze-drying. Despite being possible to control the pore size and shape by changing the parameters the interconnectivity and spatial distribution are strongly limited. These can be overcome by the rapid prototype method which can produce customized scaffold with precise and reproducible internal architecture.[6,7] The polymers are chosen based on the intrinsic properties, such as mechanical and thermal properties, chemical interaction with the solvent system, and its biological property suitable for the applications.[8]

Collagen (COL) is known to be the most promising natural material and has found diverse applications in tissue engineering due to its excellent biocompatibility and biodegradability.[9,10] However, increased biodegradation and poor mechanical

Received: May 2, 2013
Accepted: July 9, 2013
Published: July 9, 2013

  

strength limit the use of this material. Blending with another natural polymer is an effective method to modify the biodegradation rate and to optimize the mechanical properties.[11] It was recently reported that collagen−nanocomposite polymer hydrogel collagen/PLGA fiber showed potential bone[12] and nerve regeneration.[13] Chitosan (CS) is one such biopolymer widely used in a variety of biomedical fields[14] as a drug delivery vehicle, surgical thread, wound healing material, etc.[1] In combination with collagen, it exhibits enhanced mechanical and biological properties to a greater extent than the individual polymer scaffold.[4] The COL-CS biopolymer composite in gel form has also been reported to enhance the healing of dermal excision wound to a higher extent as opposed to the individual biopolymer.[15] Likewise, the mucilaginous gel of the parenchymal tissue of Aloe vera (*Aloe barbadensis Miller*) plant has been reported to have many physiologically active components that have an effective anti-inflammatory,[16] antioxidant activity,[17] and immune modulatory effect[18] that promote both tissue growth and differentiation in tissue culture.[19] It has also been reported to enhance cell proliferation[20] and has applications in treatment of burn wounds.[21,22] However, the aloe gel in combination with collagen-chitosan (COL-CS) composite scaffold has not been reported in tissue engineering. Considering the biologically active properties of this herbal material, we in this study, propose to use aloe vera gel as a component in an already reported COL-CS composite with a view to enhance the physical, thermal, and biological properties of the scaffold for tissue engineering applications.

Using the reported advantageous properties of COL-CS and aloe vera gel as such, we prepared COL-CS composite scaffold supplemented with aloe vera by freeze-drying technique and characterized by using SEM, FT-IR, DSC and TGA. Further, the biocompatibility and applicability of this novel scaffold was evaluated in vitro using 3T3 L1 fibroblast.

## 2. MATERIALS AND METHODS

**2.1. Materials.** Chitosan (80% deacetylation), Dulbecco's modified eagle's medium (DMEM), antibiotic and antimycotic solution and trypsin-EDTA solution were purchased from Sigma. Fetal bovine serum (FBS) was obtained from Pan Biotech Company. The NIH3T3 (fibroblast cells) were provided by National Centre for Cell Sciences, Pune, India. Glacial acetic acid and Dimethyl sulphoxide (DMSO) was purchased from SRL chemicals. All other reagents used were of analytical grade.

**2.2. Collagen Extraction.** Collagen type I used in this study was extracted from marine cat fish (*Tachysurus maculatus*) air bladder. The extraction was performed according to the procedure of Rose et al. (1988)[23] The purified collagen was freeze-dried and stored at −70 °C for further experimental use.

**2.3. Aloe Vera Gel Separation.** Fully matured aloe vera leaves were collected from a single garden plant, to obtain a fresh specimen for this work. The leaf rinds were removed, the clear pulp was collected, homogenized and centrifuged at 10 000 rpm for 30 min at 4 °C to remove the fibers. The supernatant, after separation, was lyophilized and stored at −20 °C until use.

**2.4. Fabrication of Porous Scaffolds.** A blend of collagen−chitosan was prepared by thorough mixing of collagen (1%) and chitosan (1%) solution in 0.05 M acetic acid in the ratio of 1:1. Similarly aloe vera blended COL-CS composite was prepared by mixing different weighed quantities of lyophilized aloe vera with the COL-CS solution to obtain final concentrations of 0.1, 0.2, 0.3, 0.4, and 0.5% (w/v) respectively. The solution blend was then poured into a 60 $mm^2$ petri dish and 24 well culture plates and left overnight in a −70 °C freezer, prior to drying by lyophilization. The composite without aloe vera was also lyophilized in the same manner and all the samples were stored at −20 °C for experimental use.

**2.5. Micro Structure Examination.** The morphology of the freeze-dried composite scaffolds was observed by using Scanning Electron Microscope (Hitachi S-3400N). The cross section of the scaffold with porous architecture was coated with Au prior to observation through SEM. The pore sizes of the scaffolds were measured using image visualization software (Image J 1.45s, NIH Image, USA). The average pore size was determined from about 20 measurements on a typical SEM image. The porosity of the scaffolds was measured by ethanol displacement method according to Guan et al (2005).[24] The porosity was calculated from the formula. The values were expressed as the mean ± standard deviation ($n$ = 3)

$$p = (v_1 - v_3)/(v_2 - v_3)$$

Where $p$ is porosity, $v_1$ indicates initial volume of ethanol in a graduated cylinder, $v_2$ represents noted volume after scaffold immersion, and $v_3$ is noted volume after scaffold removal from the immersion.

**2.6. Fourier Transform Infra Red (FTIR) spectroscopy.** Infrared spectra of scaffold specimens were obtained using an FT-IR spectrometer (ABB MB3000). Samples of each scaffold was ground and mixed thoroughly with potassium bromide at a ratio of 1:5 (sample: KBr), and an aliquot of the mixture was made into pellet. The IR spectra of the pellets were then recorded at a wavelength range of 400−4000 $cm^{-1}$ with the resolution of 0.7 $cm^{-1}$.

**2.7. Thermal Characterization.** The thermodynamic property of the scaffolds were analyzed by using Differential Scanning Calorimeter (DSC Q200) under $N_2$ atmosphere at a heating rate of 10 °C/min with the sample size of 5 mg. Pyrolytic pattern of the samples were obtained using a Thermo Gravimetric Analyzer (TGA-Q50) under $N_2$ atmosphere at a heating rate of 10 °C/min with a sample size of 5 mg.

**2.8. Swelling Studies.** Water absorption tests were conducted according to the method followed by Adekogbe & Ghanem (2005).[25] A known weight of each dry scaffold ($w_0$) was soaked separately in 0.1 M PBS, pH 7.4, at room temperature. The samples were then removed at an interval of every 10 min and the superficial water was gently blotted on a filter paper and weighed ($w_t$). The swelling ratio was calculated by using the following formula. The values were expressed as mean ± standard deviation ($n$ = 4).

$$G = (w_t - w_0)/w_0 \times 100$$

Where G is the swelling ratio, $w_0$ is the weight of the dry sample and $w_t$ is the wet weight of scaffold, after a particular soaking time, $t$.

**2.9. Mechanical Properties.** The tensile properties of the composite scaffolds were tested in an instrument of SATRA TM43 at room temperature (25 °C). Briefly, freeze- dried samples of 5 mm thickness were cut into 5 cm × 1 cm size. The gauge length between the two grips was set at 15 mm and the speed of testing was set at 5 mm/min. The values of tensile strength, strain at break and Young's modulus were determined and were expressed as the mean ± standard deviation ($n$ = 3).

**2.10. In Vitro Collagenase Degradation.** The degradation of the composite scaffolds in PBS medium containing collagenase (type I, sigma) was studied. Briefly, the scaffolds were immersed in collagenase (100 μg/mL, 28 units) containing medium and incubated at 37 °C for 5 days. The degradation was discontinued at a predefined interval, followed by centrifugation at 4000 rpm for 15 min. The clear supernatant was hydrolyzed using 6 M HCl at 110 °C for 16 h. The amount of hydroxyproline released by collagenase from the scaffold was measured spectrophotometrically.[1] The biodegradation degree is defined as the percentage of the hydroxyproline released from the scaffolds at different time to the completely degraded one with known composition and known weight. The values were expressed as the mean ± standard deviation ($n$ = 3).

**2.11. Cell Culture.** L3T3 mouse fibroblasts were cultured in a 5% $CO_2$, humid atmosphere at 37 °C in DMEM containing 10% fetal bovine serum, 100 units/ml penicillin and 100 units/ml streptomycin; the culture medium was changed every three days. For in vitro

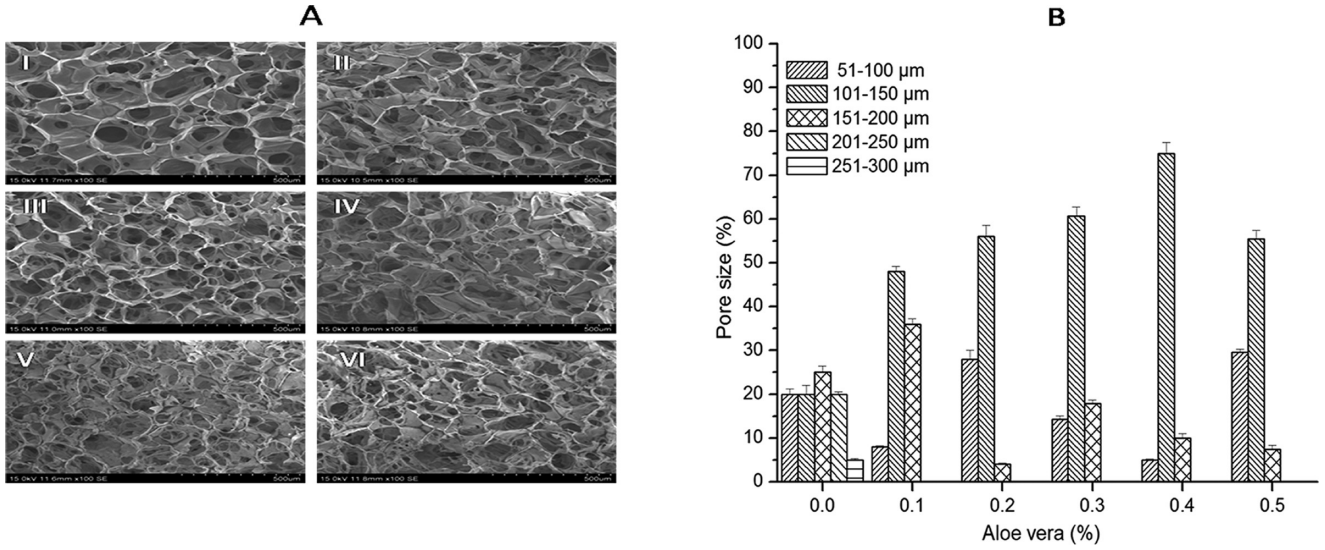


**Figure 1.** (A) SEM images of microstructures of COL-CS scaffolds on cross sections with various concentration of aloe vera viz., 0, 0.1,0.2, 0.3, 0.4, and 0.5% represented as I, II, III, IV, V, VI, respectively. (B) Percentage pore size distribution of various scaffolds from the cross- sections. Error bars represent the mean ± SD ($n$ = 3).

biocompatibility assessment, the scaffolds with 1 $cm^2$ area and 2 mm thickness were placed in 12-well culture plate. Prior to seeding with cells, the scaffold samples were sterilized under UV light for 2 h and immersed in 75% alcohol solution overnight. Afterward, the specimens were washed thrice with PBS for 30 min each, and twice with cell culture medium. L3T3 mouse fibroblasts ($3 \times 10^4$) were then seeded onto scaffolds in the culture medium, following by which cell morphology, cell compatibility, and cytotoxicity were assessed.

**2.12. Cell Viability.** MTT (3-dimethylthiazol-2,5-diphenyltetrazolium bromide) colorimetric assay was carried out to evaluate the number of viable cells after 24, 48, and 72 h of cell seeding in the presence or absence of scaffold. Briefly, cultures in the tissue culture polystyrene plate (TCP) and the test scaffolds at predetermined period were rinsed twice in PBS and then incubated with MTT solution (0.5 mg/mL in Dulbecco's medium without phenol red) at 37 °C for 4 h to allow formazan crystal formation. Later the supernatant was removed and 200 $\mu$L of DMSO was added to dissolve the formazan crystals for 30 min at 37 °C. After complete dissolution, the optical density of the supernatant solution was read at 540 nm using a micro plate reader. The wells without scaffolds were used as controls. The values were expressed as the mean ± standard deviation ($n$ = 3).

**2.13. Cell Attachment and Proliferation Studies.** The attachment and spreading nature of L3T3 mouse fibroblasts on the composite scaffolds were evaluated using SEM and Fluoroscent microscope. Cell morphology after 24 h of culture was observed in a SEM (Hitachi S-3400N). Prior to microscopical examination, cell-scaffold constructs were washed with PBS and then fixed with 4% paraformaldehyde for 4 h at 4 °C. Later, the samples were dehydrated in a series of 30, 70, 90% alcohol and freeze-dried.

The proliferation of cells in the constructs was determined using fluorescent dyes. The specimens of seeded constructs after 48 h were rinsed in sterile PBS and stained with AO/EtBr and immediately examined through fluorescence microscope (Nikon) using blue filter. AO that is able to penetrate into the intact cell binds with nucleus DNA to give green fluorescence whereas, EtBr enters through damaged membrane and binds to fragmented nucleic acid, to produce red fluorescent in dead cell.

**2.14. Statistical Analysis.** All the quantitative data were expressed as means ± standard deviations. Statistical comparisons were performed using one-way ANOVA with SPSS 13.0 for Windows software (SPSS, USA). P values of less than 0.05 were considered statistically significant.

## 3. RESULTS AND DISCUSSION

A three-dimensional COL-CS-AV composite scaffold was prepared and used in this study for cellular attachment; growth and multiplication to engineer a tissue construct using fibroblast cells. Prior to this, aloe vera gel, after lyophilization was mixed with the biopolymer blend, for functional benefits in tissue engineering, to an extent such that the tensile properties and micro structural characteristics are not affected. For this, the scaffold of COL-CS containing various concentrations of AV was analyzed to find out the optimum AV concentration at which the tensile strength is not reduced below 50% with retention of the suitable pore size.

**3.1. Microstructural Characteristics.** The microstructure of a matrix has an influence on cell attachment, proliferation, function and migration in tissue engineering. The microstructure of cross sectioned scaffolds of COL-CS and COL-CS-AV (0.1−0.5%) was studied by Scanning Electron Microscopy and the images are presented in Figure 1A. The scaffold pores were uniform and well interconnected with a mean pore size of 147.9 ± 57.8 $\mu$m for COL-CS, and sizes of 140.8 ± 26.3, 130.8 ± 25.2, 126.6 ± 28, 124.3 ± 25, and 116.8 ± 26.5 $\mu$m respectively for five different concentrations viz 0.1, 0.2, 0.3, 0.4, and 0.5% of aloe vera blended with COL-CS scaffold (Figure 1B). The scaffold porosity was found to be 86% for COL-CS followed by 89,91,92,94 and 95% for the above-mentioned concentrations of AV blended scaffold (see Figure S1 in the Supporting Information). The observation revealed that the addition of aloe vera decreased the mean pore size with increased the porosity and also caused some changes in the pore architecture. Besides pore size and its uniformity, porosity also determine the mechanical properties and the water retention property, thus the scaffold can easily absorb the culture medium to facilitate the cells for the migration, adherence and proliferation in the porous structure. AV has been reported to contain several biologically active and nutritionally important compounds such as glycoproteins, saccharides, vitamins, antioxidants., etc.[20] These compounds by virtue of their water-soluble/absorbing nature readily attract cells in the medium and promote their activities on the scaffold

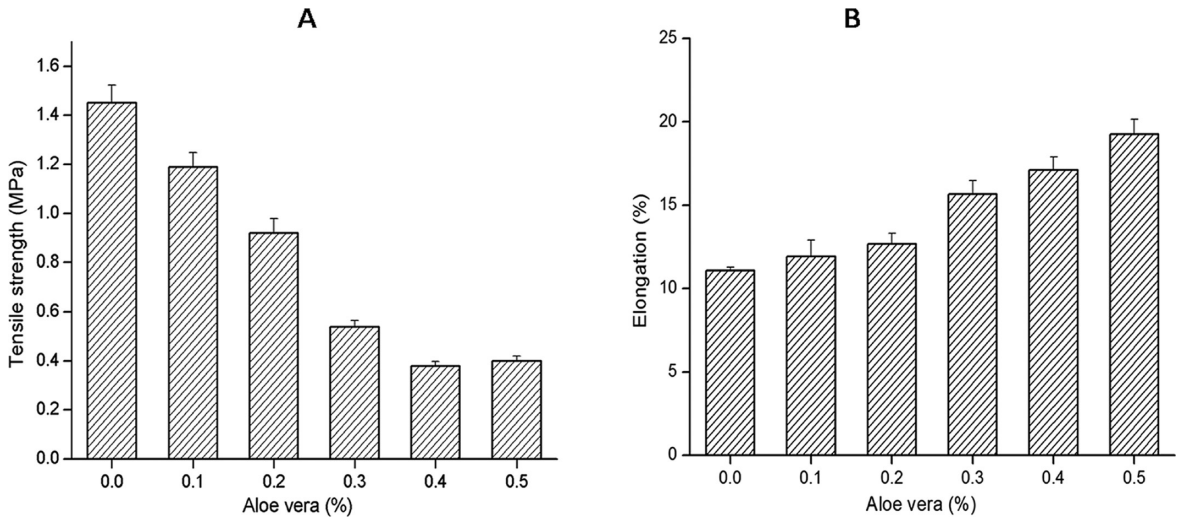


**Figure 2.** (A) Tensile strength and (B) strain at break of composite scaffolds with various concentration of aloe vera (0, 0.1, 0.2, 0.3, 0.4, and 0.5%). Error bars represent the mean ± SD ($n$ = 3).

walls. Because of the presence of these AV-borne compounds, the AV containing scaffold become flimsy upon lyophilization and therefore the pore edges bend to their sides. This change appears to reduce the pore size to some extent in COL-CS-AV scaffold (Figure 1AII-VI) compare to COL-CS alone (Figure 1AI). A 0.2% AV inclusion for instance, showed a pore size distribution of <50 $\mu$m (12%), 50−100 $\mu$m (28%), 101−150 $\mu$m (56%), and 151−200 $\mu$m (4%) compare to the AV free scaffold with pore size of <50 $\mu$m (10%), 51−100 $\mu$m (20%), 101−150 $\mu$m (20%), and 151−200 $\mu$m (25%), 201−250 $\mu$m (20%), 251−300 $\mu$m (5%). Therefore, it is quite obvious that the pore size also could be one of the reasons for the enhanced cellular activity observed in this study.

**3.2. Mechanical Properties.** The tensile data of the COL-CS scaffold blended with various concentrations (0.1, 0.2, 0.3, 0.4 and 0.5% (w/v) of aloe vera are presented in Figure 2A. The AV free scaffold displayed a tensile strength of 1.5 MPa while its inclusion gradually decreased the scaffold strength depending upon the concentration of the former. For instance, the tensile properties of the scaffolds with uniform thickness and material content in one unit area is varying in nature as AV is the determining factor. Percent reduction in the tensile value decreased to 79, 64, 36, 29, and 21 respectively for 0.1, 0.2, 0.3, 0.4, and 0.5% w/v AV incorporation. The concentration of AV at which 50% strength was lost is considered as effective concentration ($EC_{50}$), which according to this study falls between 0.2% and 0.3% therefore, it was decided to have 0.2% as optimum concentration. The COL-CS composite blend exhibited maximum tensile strength which was due to the H-bond/ionic interaction between their functional groups viz −OH, −COOH and $-NH_2$ of collagen and the −OH and $-NH_2$ groups of chitosan. Despite this, the presence of lyophilized aloe vera gel affects the tensile strength. This may be due to the interference of its functional groups in the COL-CS interaction, apart from its hydrophilic nature. Contrary to the strength property, the elongation property increased with respect to increasing AV concentration. (Figure 2B) suggests that the AV gel imparts elasticity to COL-CS composite scaffold. In other words, the porous scaffold possesses low strength but it is of high extensibility which is a function of pore orientation and interconnection. The SEM examination confirmed that the presence of AV at a concentration of >0.2% leads to disuniformity of pores and disturbance in the structural architecture. This ultimately would contribute to destabilization of structural integrity of the scaffold in an aqueous medium. Hence a 0.2% AV containing scaffold was chosen for further characterization and in vitro studies.

**3.3. FT-IR.** For a biological composite system containing three types of materials, Fourier Transform Infra Red spectroscopy could be used as an effective method to define the existence of each component. The FTIR spectra of COL, CS, COL-CS, and COL-CS-AV scaffolds were obtained separately and are shown in Figure 3. The FTIR spectrum of

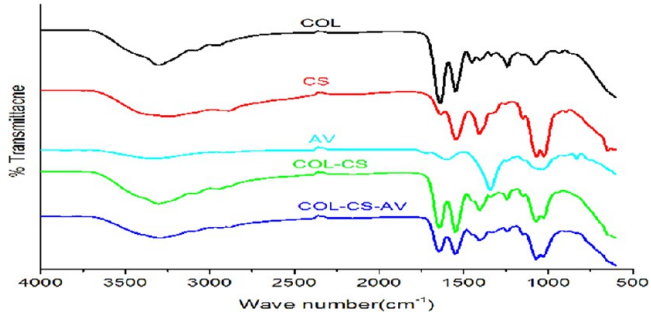


**Figure 3.** FTIR spectra of COL, CS, AV, COL-CS, and COL-CS-AV.

collagen scaffold displayed the characteristic absorption band in the region of 1639 $cm^{-1}$ (C═O stretch) for amide I; 1547 $cm^{-1}$ (N−H Bend) for amide II; 1239 $cm^{-1}$ for amide III; other bands at 3302 $cm^{-1}$ for O−H stretch; 2951 $cm^{-1}$ for aliphatic groups ($-CH_2$ and $-CH_3$); and 1451 $cm^{-1}$ for $-COO^-$.

The Chitosan spectrum exhibiting the absorption band in the region of 3298 $cm^{-1}$ represents the O−H stretch, 1636 $cm^{-1}$ for C═O stretch of amide I, and 1546.3 $cm^{-1}$ for N−H stretch of amide II.

Aloe vera showed the absorption band around 3314 $cm^{-1}$, which may be due to the presence of hydrogen bonded N−H stretching, characteristic of amino acids. The absorption band at 2920 $cm^{-1}$ is due to the symmetrical and asymmetrical C−H stretching of the $-CH_2$ groups. This band is also characteristic of the presence of aliphatic (−CH) groups in these compounds. The absorption band at 1719 $cm^{-1}$ is characteristic of C═O

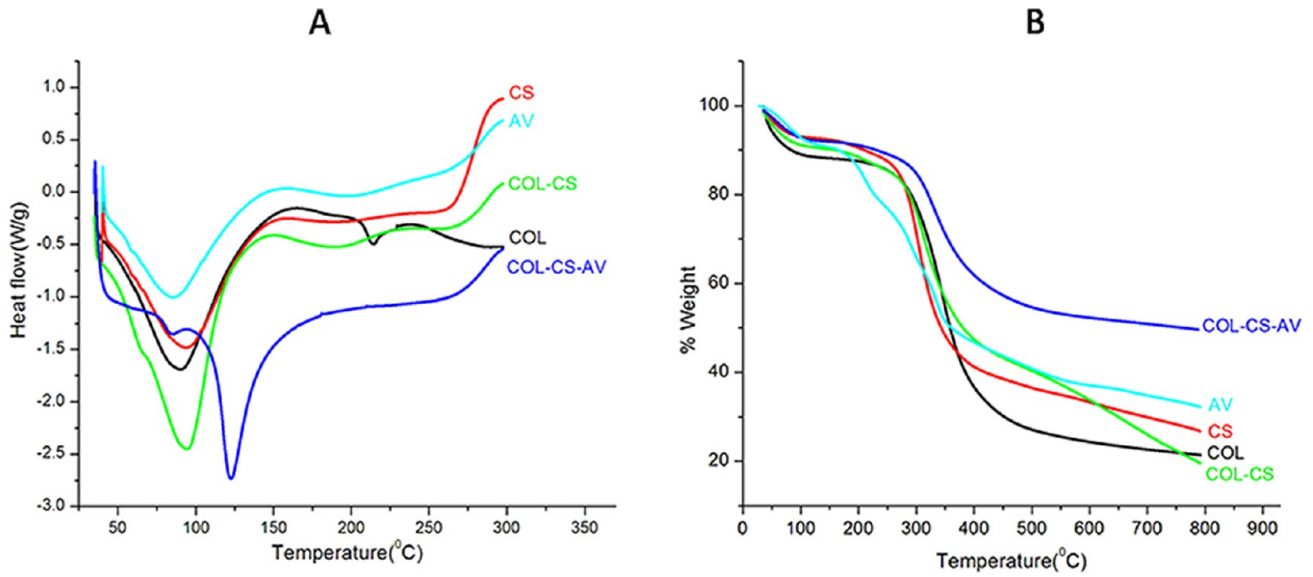


**Figure 4.** (A) Differential scanning calorimetric and (B) thermogravimetric analysis of various scaffolds COL, CS, AV, COL-CS, and COL-CS-AV.

stretching and indicates the presence of carbonyl groups. The strong absorption band at 1580 $cm^{-1}$ is due to C═C stretching, which indicates the presence of vinyl ether and aloin compound. The absorption band at 1242 $cm^{-1}$ is due to the stretching vibrations of C−O groups of esters and phenols. The strong absorption band at 880 $cm^{-1}$ is due to the C−H out of plane deformation.[26]

COL-CS spectrum showed the characteristic absorption band in the region of 3314 $cm^{-1}$ (O−H stretch), 1695 $cm^{-1}$ (C═O stretch) amide-I, 1563 $cm^{-1}$ (N−H bending) amide II, and 1299 $cm^{-1}$ amide III. The interactions between collagen and chitosan may occur by the formation of H bonds. The −OH groups and $-NH_2$ groups in collagen are capable of forming hydrogen bonds with −OH and $-NH_2$ groups in chitosan. Moreover, the −C═O groups and $-NH_2$ groups in collagen may also form hydrogen bonds with −OH and $-NH_2$ groups in chitosan. Additionally, ionic bonds may be formed between collagen and chitosan. These molecules are capable of forming a complex with oppositely charged ionic polymers, and these interactions may form polyanionic−polycationic complex.[27] But the evidence of FT-IR spectra here does not indicate the formation of new polyanionic−polycationic complex between collagen and chitosan, obviously, because of their same main functional groups.

The spectrum of aloe vera blended scaffold (COL-CS-AV) showed a shift from 3314 to 3281 $cm^{-1}$, which may be due to the hydrogen bond formation between the polysaccharide of aloe vera and the −OH and $-NH_2$ groups in collagen or chitosan. Appearance of new sharp absorbance peak at 1628 $cm^{-1}$ may be due to the formation of amide or ester linkages between the amino groups of aloe vera and carboxyl group of collagen. The shift of amide peak from 1563 $cm^{-1}$ (obtained for AV) to 1530 $cm^{-1}$ for AV blended scaffold may be due to the influence of aloe vera. Similarly a prominent sharp ester peak was observed at 1226 $cm^{-1}$ which is due to the stretching vibrations of C−O groups of esters and phenols which was absent in COL-CS spectrum. The absorption peak at 1119 $cm^{-1}$ is due to the C−O stretch of polysaccharides of aloe vera which was absent in COL-CS spectrum. The vital observation from this study is that the blending of collagen, chitosan and aloe vera did not make a significant change in the chemical property. Hence, they can exert their characteristics individually during in vitro culture studies. Thus the cells can avail the properties of individual components.

**3.4. Thermodynamic Property.** Figure 4A shows the DSC pattern of collagen, chitosan, aloe vera gel, and their blend scaffold. The characteristic endothermic peaks represent the temperature of dehydration ($T_D$) of individual biomaterials in an environment of nitrogen. The $T_D$ values along with the enthalpy of dehydration ($\Delta H_D$) obtained from DSC measurements are listed in Table 1A. These DSC results clearly indicate

**Table 1A. Thermal Properties of Various Scaffolds**

| | scaffold | | | | |
|---|---|---|---|---|---|
| | collagen | chitosan | AV | COL-CS | COL-CS-AV |
| $T_D$ (°C) | 90.10 | 94.95 | 86 | 94.62 | 122.44 |
| $\Delta H_D$ (J/g) | 437.5 | 347.4 | 274 | 525.6 | 209 |

that $T_D$ values of collagen or chitosan are comparable to that of COL-CS composite scaffold because of the fact that the collagen super coil structure seems to be stabilized by the involvement of chemical forces contributed by collagen−chitosan interactions. In this blend, the formation of hydrogen bonds between these two macromolecules competes with the formation of hydrogen bonds between molecules of the same polymer.[9] Interestingly, in COL-CS-AV system, AV also participates in the process of intermolecular interaction involving all three constituents and contributes to the increased $T_D$ (124.36 °C) compared to other systems. On the other hand, unlike the $T_D$ values, the $\Delta H_D$ values for collagen (766.6 J/g) and chitosan (596.3 J/g) showed a clear difference due to their individual molecular composition and structural conformation. However, the blending of CS with COL did not exhibit any negative effect on the $T_D$ value (Table 1A). This observation suggests that CS at a concentration equal to that of collagen does not affect the pyrolytic property but stabilizes the super coil structure as evidenced by the increased $\Delta H_D$ values of the sample in solid state (lyophilized condition). Therefore the higher $\Delta H_D$ value exhibited for collagen or COL-CS system compared to chitosan alone is due to the increased energy required to uncoil the collagen superstructure. Contrarily, the


dx.doi.org/10.1021/am401637c | ACS Appl. Mater. Interfaces 2013, 5, 7291−7298

AV blended COL-CS composite which required much lesser energy which is represented by a much narrower endothermic peak, compared to other systems, reveals the highly susceptible nature of the collagen superstructure, more particularly in the presence of AV, than that of CS. At the same time, DSC data also showed a shift in the $T_D$ values of COL-CS especially in the presence of AV system. This obviously indicates the AV induced collagen structural reorganization and subsequent increase in resistance to pyrolysis by the AV (polysaccharide) containing composite biomaterial.

The disorganization of collagen structure as observed by decreased $\Delta H_D$ values in AV additive environment may be due to the partial destabilization of the intramolecular hydrogen bonds of the protein in the given experimental condition (when $T_D$ = 124.36 °C). However below this temperature, the AV blended COL-CS must be intact and therefore can be safely stored at ambient temperature for its application. Nevertheless, a biomaterial with partially destabilized collagen structure would still be advantageous as it would be able to absorb more water molecules into its structure. Such a hydrated material could serve as a better scaffold in Tissue engineering applications.

The above facts are further justified by the results of TGA (Figure 4B). Presented in Table 1B are the values of weight loss

**Table 1B. % Weight Loss of Various Scaffolds in Different Stages**

| scaffold | peak max temp (°C) | % weight loss 35−200 °C | 200−400 °C | 400−700 °C |
|---|---|---|---|---|
| COL | 344.83 | 11.41 | 51.04 | 13.85 |
| CS | 303.97 | 10.01 | 48.78 | 11.30 |
| AV | 276.68 | 13.95 | 39.10 | 12.00 |
| COL-CS | 313.77 | 11.01 | 41.09 | 16.37 |
| COL-CS-AV | 331.75 | 8.55 | 29.09 | 12.27 |

obtained by thermogravimetry for COL, CS, COL-CS, and COL-CS-AV samples. The weight loss in the samples occurred in three stages: the first one refers to the loss of structural water molecule of the scaffold (25−200 °C); second, because of the thermal degradation of the polymers (200−400 °C); and the third stage (400−700 °C) is attributed to the carbonization of polymeric material.[28] It is observed that the COL-CS scaffold exhibited weight loss of 41% in the transition temp of 200−400 °C compared to 51% for collagen and 48.8% for CS, individually. However, COL-CS-AV showed a weight loss of only 29%, which is much lower compared to other scaffolds. This shows that the aloe vera may have had much stronger interactions with COL-CS and thus increased the thermal stability.

**3.5. Swelling Studies.** Percent swelling of different scaffold preparations with or without AV at different intervals of water contact time is depicted in Figure 5. The swelling of COL-CS increased rapidly to 250% in the initial 10 min time interval and reached a saturation of 350% in 40 min. Blending of 0.1% aloe vera with COL-CS increased the swelling to 300% in 10 min and a saturation of 400% in 40 min. Similarly the swelling percent gradually increased with increasing aloe vera concentration from 0.1% to 0.5%. This again may be due to the hydrophilic property of aloe vera polysaccharide that is included in the COL-CS composite scaffold. At equilibrium

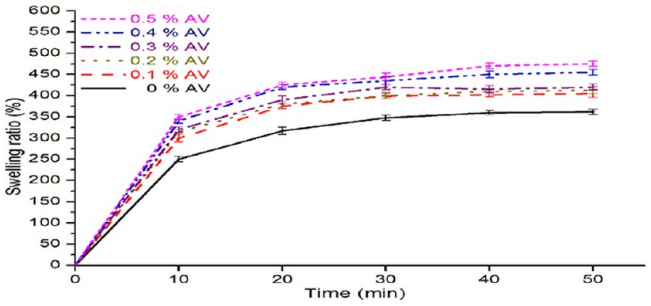


**Figure 5.** Swelling properties of COL-CS scaffold containing different concentration of aloe vera (0−0.5%). Error bars represent the mean ± SD ($n$ = 4).

of swelling, the composite scaffold containing >0.2% AV gel resulted in loss of shape and structural integrity owing to the highly hydrophilic nature of the AV gel. This property probably could have led to weakening of collagen intramolecular interaction as well as the intermolecular interactions between collagen and chitosan. Based on these observations, the optimum concentration of lyophilized AV gel to be used in the COL-CS scaffold was fixed as 0.2% w/v. High water holding capacity of such a scaffold is favorable for cell adhesion and growth. Also, the water holding property would facilitate easy transport of nutrients from the scaffold to cells in the culture system. In wound healing, this would prevent the fluid loss from the body when applied on the wound at the wound site.

**3.6. In Vitro Biodegradation.** Figure 6 compares the degree of biodegradation of COL-CS scaffold with and without

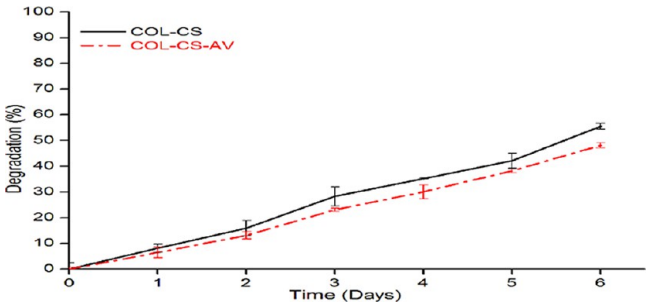


**Figure 6.** In vitro collagenase degradation of COL-CS scaffold without and with (0.2%) AV. Error bars represent the mean ± SD ($n$ = 3).

aloe vera gel. The linear curve obtained clearly demonstrates the controlled degradation of collagen and release of hydroxyproline in an increasing order with respect to time. On day 1, a degradation of 6.5% in COL-CS-AV and 8% in COL-CS was observed; whereas on day 6 of the experiment, it was 48 and 55% of weight loss respectively for scaffolds with and without aloe vera. Overall, the rate of biodegradation increased as a function of time in both the scaffolds. However, the COL-CS-AV showed lesser biodegradation compared to COL-CS scaffold. This may be attributed to the presence of aloe vera which is likely to reduce the accessibility of enzymes to the vulnerable sites in the collagen molecule. Additionally, AV influenced weakening of chemical forces of collagen−chitosan interaction leads to more disturbances in porous architecture with increasing AV concentration and hence results in poor mechanical properties. This shows that the degradation

rate of the collagen-based scaffold can be modified by incorporating aloe vera to an appropriate level.

**3.7. Cell Viability.** Biocompatibility of the composite scaffolds was evaluated using MTT assay. This assay measures the metabolic activity of the cells, which can be correlated with the number of viable cells. The results of cell viability by this assay were compared with the control group as shown in Figure 7. The results elucidate the increase in cell numbers with

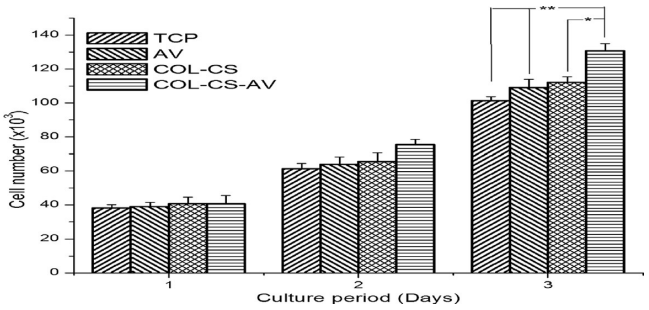


**Figure 7.** MTT assay of fibroblast cells cultured on COL-CS, COL-CS-AV, and TCP. Error bars represent the mean ± SD ($n$ = 3; *denotes statistically significant difference, $p < 0.05$, ** denotes $p < 0.01$).

respect to time from day 1 to 3. The viability of cells in medium containing COL-CS-AV composite scaffold was almost equal to that of COL-CS, AV and control, and there was no significant difference between them ($p > 0.05$) on day 1. This indicates that the viability was not affected by addition of aloe vera to COL-CS scaffold. On day 3, there was a significant increase in cell population in COL-CS-AV group that may be due to glycoproteins in the aloe vera gel that are reported to stimulate the cell proliferation[29] and promote the growth in the case of human fibroblast,[30] whereas anthroquinones (aloe-emodin) exhibit antioxidant and free radical scavenging property.[31] Additionally, the increased hydrophilic property of scaffold due to the presence of AV gel allowed the scaffold to swell in the culture medium and facilitate the cell infusion into the 3D structure, followed by attachment and growth. The increased swelling also allows the scaffold samples to avail nutrition from culture media more effectively.[2] Thus the inclusion of AV in COL-CS scaffold resulted in altered biological property that favored the establishment of a conducive environment for cell adhesion, growth and proliferation.

**3.8. Cell Morphology and Proliferation on Scaffolds.** The topography and porosity of a scaffold play a significant role in the attachment and the proliferation of mammalian cells.[2] Biocompatibility results of the aloe vera blended COL-CS composite scaffold as evaluated by SEM and fluorescent Microscopy are presented in panels A and B in Figure 8, respectively. The SEM image demonstrated that the cells were attached to the scaffolds and spread to occupy the surface of the pore walls to accumulate ECM. However, there was a clear difference in the appearances between the scaffolds with and without AV: on the AV-containing COL-CS scaffolds, there was a high degree of cellular recruitment and attachment on its surface because of the flabbiness of the biomaterial, and at a later stage, they grew in multilayers and secreted ECM with filopodial extension as seen in the SEM image in Figure 8AII. This observation was supported by the results fluorescent microscopy (Figure 8BII), where the cell density inside the COL-CS-AV scaffold was relatively more and interconnected

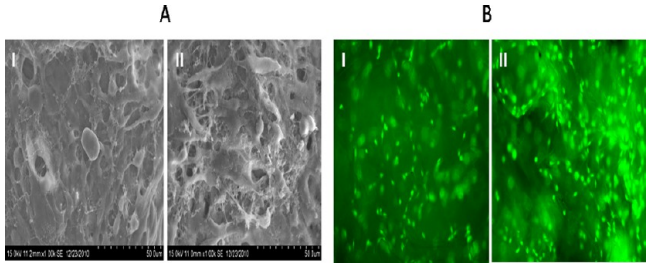


**Figure 8.** (A) SEM micrographs (1000×) of fibroblast cells after 4 days of culture on composite scaffolds: (I) COL-CS, (II) COL- CS-AV. (B) Fluorescence micrograph (20 ×) of fibroblast cells after 5 days of culture on (I) COL-CS, (II) COL-CS-AV scaffolds.

than in COL-CS. This confirmed that the aloe vera facilitated the cell migration[32] into the scaffold and enabled their easy adherence on porous wall and thus augmented cellular proliferation that leads to aggregation. All these observation are attributable to the bioactive nature of the AV because of its chemical composition. This would subsequently enhance cell–cell signaling and tissue formation.[33] Further, glucomannan, a mannose-rich polysaccharide and the most common polysaccharide present in AV gel, interacts with growth factor receptors on the fibroblast, thereby stimulating its activity and proliferation, which in turn significantly increases collagen synthesis, which is major component of extra cellular matrix (ECM) and favors more cell adherence on the scaffold.[34,35]

## 4. CONCLUSION

In conclusion, a versatile 3D scaffold consisting of fish collagen, chitosan and aloe vera prepared in this study possesses all requisite physical and biological properties to recruit, attach, and proliferate the fibroblasts. The inclusion of AV to the COL-CS composite imparts novelty to this study, as the latter provides structural support, whereas the former offers extra-nutritional support. Considering the overall physiochemical and biological properties of the AV blended COL-CS scaffold, this could be advantageously used as a promising biomaterial for tissue engineering.

## ■ ASSOCIATED CONTENT

### Ⓢ Supporting Information

Porosity measurement of COL-CS scaffolds with various concentration of aloe vera. This material is available free of charge via the Internet at http://pubs.acs.org.

## ■ AUTHOR INFORMATION

### Corresponding Author

*E-mail: chellanrose@yahoo.co.uk or rose@clri.res.in. Tel: + 91-44-24430273, Fax: + 91-44-24911589.

### Notes

The authors declare no competing financial interest.

## ■ ACKNOWLEDGMENTS

The Council of Scientific and Industrial Research (CSIR), Ministry of Science and Technology, Government of India, New Delhi, India, is being acknowledged, with profound gratitude, for supporting this research by rendering the required financial assistance through a fellowship to the first author.

## REFERENCES


(1) Ma, L.; Gao, C. Y.; Mao, Z. W.; Zhou, J.; Shen, J. C.; Hu, X. Q.; Han, C. M. *Biomaterials* **2003**, *24*, 4833−4841.
(2) Peter, M.; Ganesh, N.; Selvamurugan, N.; Nair, S. V.; Furuike, T.; Tamura, H.; Jayakumar, R. *Carbohydr. Polym.* **2010**, *80*, 687−694.
(3) Lu, Q. J.; Ganesan, K.; Simionescu, D. T.; Vyavahare, N. R. *Biomaterials* **2004**, *25*, 5227−5237.
(4) Arpornmaeklong, P.; Pripatnanont, P.; Suwatwirote, N. *Int. J. Oral. Maxillofac. Surg.* **2008**, *37*, 357−3566.
(5) De Santis, R.; Gloria, A.; Russo, T.; D'Amora, U.; Zeppetelli, S.; Dionigi, C.; Sytcheva, A.; Herrmannsdoerfer, T.; Dediu, V.; Ambrosio, L. *J. Appl. Polym. Sci.* **2011**, *122*, 3599−3605.
(6) Gloria, A.; Causa, F.; Russo, T.; Battista, E.; Della Moglie, R.; Zeppetelli, S.; De Santis, R.; Netti, P. A.; Ambrosio, L. *Biomacromolecules* **2012**, *13*, 3510−3521.
(7) Domingos, M.; Chiellini, F.; Gloria, A.; Ambrosio, L.; Bartolo, P.; Chiellini, E. *Rapid Prototyping J.* **2012**, *18*, 56−67.
(8) Weigel, T.; Schinkel, G.; Lendlein, A. *Expert. Rev. Med. Devices* **2006**, *3*, 835−851.
(9) Chen, Z.; Mo, X.; He, C.; Wang, H. *Carbohydr. Polym.* **2008**, *72*, 410−418.
(10) Faikrua, A.; Jeenapongsa, R.; Sila-asna, M.; Viyoch, J. *ScienceAsia* **2009**, *35*, 247−254.
(11) Taravel, M. N.; Domard, A. *Biomaterials* **1993**, *14*, 930−938.
(12) Fu, S.; Ni, P.; Wang, B.; Chu, B.; Zheng, L.; Luo, F.; Luo, J.; Qian, Z. *Biomaterials* **2012**, *33*, 4801−4809.
(13) Ouyang, Y.; Huang, C.; Zhu, Y.; Fan, C.; Ke, Q. *J. Biomed. Nanotechnol.* **2013**, *9*, 931−934.
(14) Lionzo, M. I.; Lorenzini, G. C.; Tomedi, J.; Pranke, P.; Silveira, N. P. *J. Biomed. Nanotechnol.* **2012**, *8*, 337−344.
(15) Judith, R.; Nithya, M.; Rose, C.; Mandal, A. B. *Biologicals* **2012**, *40*, 231−239.
(16) Vazquez, B.; Avila, G.; Segura, D.; Escalante, B. *J. Ethnopharmacol.* **1996**, *55*, 69−75.
(17) Hu, Q. H.; Hu, Y.; Xu, J. *Food. Chem.* **2005**, *91*, 85−90.
(18) Vijayalakshmi, D.; Dhandapani, R.; Jayaveni, S.; Jithendra, P. S.; Rose, C.; Mandal, A. B. *J. Ethnopharmacol.* **2012**, *141*, 542−546.
(19) Saibuatong, O. A.; Phisalaphong, M. *Carbohydr. Polym.* **2010**, *79*, 455−460.
(20) Seongwon, C.; Myung, H. C. *Semin. Integr. Med.* **2003**, *1*, 53−62.
(21) Somboonwong, J.; Duansak, N. *J. Med. Assoc. Thailand* **2004**, *87*, 69−74.
(22) Maenthaisong, R.; Chaiyakunapruk, N.; Niruntraporn, S.; Kongkaew, C. *Burns* **2007**, *33*, 713−718.
(23) Rose, C.; Kumar, M.; Mandal, A. B. *Biochem. J.* **1988**, *249*, 127−133.
(24) Guan, J. J.; Fujimoto, K. L.; Sacks, M. S.; Wagner, W. R. *Biomaterials* **2005**, *26*, 3961−3971.
(25) Adekogbe, I.; Ghanem, A. *Biomaterials* **2005**, *26*, 7241−7250.
(26) Ravi, S.; Kabilar, P.; Velmurugan, S.; Ashok Kumar, R.; Gayathiri. *J. Exp. Sci* **2011**, *2*, 10−13.
(27) Sionkowka, A.; Wisniewski, M.; Skopinska, J.; Kennedy, C. J.; Wess, T. J. *Biomaterials* **2004**, *25*, 795−801.
(28) Horn, M. M.; Martins, V. C. A.; Plepis, A. M. D. *Carbohydr. Polym.* **2009**, *77*, 239−243.
(29) Yagi, A.; Egusa, T.; Arase, M.; Tanabe, M.; Tsuji, H. *Planta Med.* **1997**, *63*, 18−21.
(30) Danof, I. E.; McAnalley, W. *Drug Cosmetic Ind.* **1983**, *133*, 105−106.
(31) Malterud, K. E.; Farbrot, T. L.; Huse, A. E.; Sund, R. B. *Pharmacology* **1993**, *47*, 77−85.
(32) Fray, T. R.; Watson, A. L.; Croft, J. M.; Baker, C. D.; Bailey, J.; Sirel, N.; Tobias, A.; Markwell, P. J. *J. Nutr.* **2004**, *134*, 2117S−2119S.
(33) Neves, S. C.; Teixeira, L. S. M.; Moroni, L.; Reis, R. L.; Van Blitterswijk, C. A.; Alves, N. M.; Karperien, M.; Mano, J. F. *Biomaterials* **2011**, *32*, 1068−1079.
(34) Surjushe, A.; Vasani, R.; Saple, D. G. *Indian. J. Dermatol.* **2008**, *53*, 163−166.
(35) Chithra, P.; Sajithlal, G. B.; Chandrakasan, G. *Mol. Cell. Biochem.* **1998**, *181*, 71−76.